ARTICLE

Calcium oxalate crystallization in synthetic urinary medium: the impact of resorcinares and calixarenes

Received 00th January 20xx,
Accepted 00th January 20xx

DOI: 10.1039/x0xx00000x

Odin Bottrill[a], Matthew Boon[a], Franca Jones[a]*, Mauro Mocerino[a]

Kidney stones are an ailment that effects many people globally. While kidney stones can sometimes be treated with simple dietary changes this does not solve all cases. Most kidney stones are comprised predominantly of calcium oxalate and there few very options in terms of accepted treatments for patients who suffer from this reoccurring condition. This research investigates the use of additives, resorcin[4]arenes and calix[4]arenes functionalised with three different amino acids (lysine, aspartic acid and proline) and their impact on the nucleation, morphology and zeta potential of calcium oxalate in a synthetic urine environment. The resorcin[4]arene functionalised with aspartic acid showed the stabilisation of calcium oxalate dihydrate rather than calcium oxalate monohydrate typically observed. The calix[4]arenes functionalised with proline and lysine showed large impacts on the morphology of the crystals formed. Additionally, the additives show significant impacts on the zeta potential of the crystals formed. It was also discovered that all three additives show evidence of incorporation to different extent through the crystal. These impacts were only observed when the macrocycles functionalised with amino acids were present as the free amino acids showed minimal impact.

Introduction

Biomineralisation is an evolutionary response by organisms utilised for a number of purposes, ranging from formation of skeletons to gravitaxis. (1) However, biomineralisation can also be pathological; for example, leading to the uncontrolled formation of kidney stones. In the case of kidney stones, calcium oxalate is known to be the main species (70% of cases). (2) Kidney stones are mainly made of whewellite or calcium oxalate monohydrate (COM, $CaC_2O_4 \cdot H_2O$) and/or whedellite or calcium oxalate dihydrate (COD, $CaC_2O_4 \cdot (2 + x)H_2O$ with $x \leq 0.5$), though this hydrate is less stable in the medium. (3) There is also calcium oxalate trihydrate or caoxite (COT, $CaC_2O_4 \cdot (3\text{-}x)H_2O$ with $x < 0.5$), although this is not observed due to its very low thermodynamic stability in the medium.

The pathology of kidney stones brings into question how can this process be controlled or mitigated? A field of research focused around this is that of crystal growth modifiers. *Crystal growth modifier* is a general term for a species that can alter some aspect of the crystal's formation. Crystal growth modifiers are chemicals (that can be referred to as additives) that can affect the crystal size, shape or nucleation rate of particles. One possible mechanism of modification is through the chelation of one of the crystal's constituents in solution, lowering the supersaturation. Alternatively, the additive could bind to the surface of the crystal, resulting in the slowing or prevention of growth at the binding sight, effecting the morphology. (4) Once adsorbed to the surface the additive can also effect the zeta potential around the particle and thereby impact the possibility of aggregation. (5) Additives could also stabilise other polymorphs or hydrates through methods such as templating. (6) Templating is a method whereby a large molecule interacts with the crystal, forming an interface that directs and controls the crystal's formation and can cause selective formation of hydrates and polymorphs. (7) Incorporation of the additive is also possible, where the additive is internal to the crystal resulting in an altering in the crystal's behaviour and growth. There has already been some research into the use of crystal growth modifiers for the control of the formation of kidney stones, (8-21) although many of the studies investigate the impact in simple solutions unrelated to real life conditions.

In the case of kidney stone formation in urine some aspects of the development of stones are well explored. Generally, the accepted mechanism of stone formation begins with the supersaturation of cation and anion that then undergoes nucleation. The crystal then interacts with the cells in the kidneys, holding the stone in place and allowing the stone to grow larger over time. (22) During the formation of the stone there are a large number of organic species ranging from small organics to proteins present in the urine which can interact with or incorporate into the crystal. Analysis of calcium oxalate stones has shown the crystal's internal matrix can consist of a number of other smaller molecules and proteins. (23) It is still contentious in the literature if these proteins play a role in the inhibition or promotion or are simply incorporated during the crystallisation phase.

[a] *School of Molecular and Life Sciences, Curtin University, Kent Street, 6152, Perth Western Australia.*

Electronic Supplementary Information (ESI) available: Synthetic methods, SEM images, optical images, Raman Spectra. See DOI: 10.1039/x0xx00000x

There are some options for patients for the removal of kidney stones. However, treatment of the condition as a re-occurring disease is largely absent. There is some interest in the possible treatment of the condition using citric acid (or derivatives) and phosphates from literature. (24) Additionally, it is recommended patients who are reoccurring stone formers undergo dietary changes to prevent the intake of the relevant species causing the condition. Due to the limited treatment options for reoccurring stone formers new chemicals must be tested and researched as possible therapeutics to prevent or inhibit the continued formation of these stones. Much of the research associated with additives is restricted to smaller molecules (or some identified proteins in the urine) and little has been done with larger molecular additives.

Calixarenes have been widely used for many purposes from medicinal to imaging. (25-28) The reason for the variety of uses is due to the amount of freedom the base structure has for functionalisation (Figure 1a). Another advantage is within the circular structure itself, as it keeps the functional groups in a well-defined location, for example, with groups all on the upper rim of the circular structure and at known distances. This not only aids in the interpretation of results but also allows the functional groups to have strong interactions as the presence of the functional groups on one side of the scaffold can lead to more favourable binding between the molecule and the crystal surface.

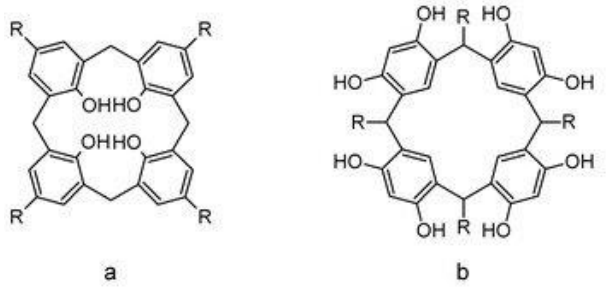

Figure 1. Generalised structure of (a) calix[4]arenes and (b) resorcin[4]arenes (17)

There has been much research in terms of the synthesis of novel calixarenes, although many of these only get tested for few purposes. (29) The aim of this research is to observe the impact of calixarenes and resorcinarenes on calcium oxalate crystallization and to guide this avenue of research for the future (and ultimately to new therapeutics). This work expands on earlier research on possible inhibitors using smaller molecules using the same synthetic urinary medium (SUM) and methods (30) whilst also expanding on research into calixarenes as crystal growth modifiers. (28, 31) More specifically, this work will look at the functionalisation of these base structures with amino acids (aspartic acid, lysine and proline) and observe the impact that the molecule has on the formation of calcium oxalate nucleation and formation. The impact of the molecules will then be compared to the relevant amino acid to see the impact that having those amino acids attached to the large organic scaffold has on the observed crystals. In addition, the impact of zinc ions was also investigated. Zinc ions are normally present in urine and have been found to have a complex impact on calcium oxalate crystallisation (32). Finally, it should be stressed that even this SUM is not a true synthetic urine but is closer to reality than matching the ionic strength with NaCl due to the presence of commonly found ions such as magnesium and phosphate.

Materials and Methods

Materials

All reagents were of analytical grade quality, or they were used as synthesised. The water present or added in all the experiments and stock solutions was deionised water. A stock solution of the SUM was prepared at 10 times the concentration as reported in a previous paper, shown in (**Table 1**) and adjusted to a pH of 6.5 with hydrochloric acid. (30) Potassium phosphate monobasic was stored separately to avoid phosphate precipitation occurring in the SUM. To avoid bacterial growth in the SUM, sodium azide (1% w/w) was added. CAUTION: sodium azide is hazardous and should be handled according to Safety Data Sheet instructions.

Table 1. Stock solution of synthetic urinary medium (SUM) adapted from (33)

Species	Concentration (mM)
Sodium Chloride	105.50
Potassium Chloride	63.70
Ammonium Chloride	27.60
Magnesium Sulfate	3.95
Potassium Phosphate Monobasic*	3.23
Sodium Citrate	3.21

*stock solution kept separate from other SUM species

Zinc ions are also present in urine and as such the interaction of zinc ions with SUM was tested by adding zinc chloride. Thus, the SUM with zinc ions is a more physiologically comparable SUM. The zinc chloride solution stock solution (0.1M) was kept separate from the SUM solutions and was added into the medium such that the final concentration was 1 mM, which is within the normal range for human urine. (34) Each of the organic inhibitors investigated is shown in **Table 2.** The synthesis procedure and characterisation of the calixarenes and resorcinarene molecules can be found in the supplementary information.

Table 2. List of organic compounds tested in this work

Chemical structure	pI of amino acid (isoelectric point)	Molecular Weight (g/mol)	Name/Purity
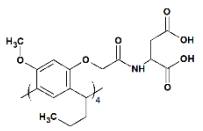	-	1405.392	Aspartic acid functionalised propyl resorcin[4]arene (PRAsp) Purity by NMR (>95%)
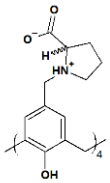	-	933.04	Proline functionalised calix[4]arene (CPro) Purity by NMR (>95%)
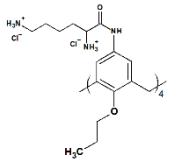	-	1457.24	Lysine functionalised propyl calix[4]arene (PCLys) Purity by NMR (>95%)
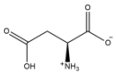	2.77	133.11	L-Aspartic Acid (Asp) Acros Organics (>98%)
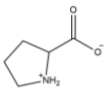	6.3	115.13	L-Proline (Pro) BDH Biochemical (>98%)
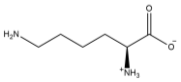	9.74	146.19	L-Lysine (Lys) Sigma Aldrich (>99%)

Morphological tests

A 20 mL solution was prepared by using deionised water, 2 mL of the SUM stock solution and 2 mL of phosphate monobasic stock solution. Sodium oxalate solution 0.4 mL, 0.1 M was then added. A clean glass disk of 0.5 cm radius was added to the vial to allow for analysis of the solids formed. The additive (Table 2) was then added at the desired concentration. The calixarenes and resorcinarenes were tested at concentrations of 1 mM while the amino acids were tested at 4 mM to account for the macrocycles containing 4 equivalents of the amino acid in the structure. Deionised water was added, if required, to ensure that the final volume was 20 mL for all experiments. The mixture in the vial was left for 15 to 20 minutes until the temperature equilibrated to 37 °C before adding 0.4 mL, 0.1 M of calcium chloride to commence the crystallization process. This solution was left for 18 to 24 hours after which the glass disk was collected, washed gently with water, and dried.

In the cases where zinc ions were added to the medium, zinc chloride was present at a final concentration of 1 mM for all tests and added prior to the calcium chloride addition. This concentration was chosen as it is within the normal concentration range for human urine. (34)

The recovered glass disks were then analysed by Raman spectrometry using a WITec alpha 300SAR (Bruker) to determine the hydrate form. The Raman functionality utilises a frequency-doubled NdYAG laser of wavelength 532 nm (green) of 50 mW power with silicon being used as the reference material.

After observing the effects of the additives on the crystals using the optical microscope and Raman spectroscopy, the disks were placed on carbon coated scanning electron microscope (SEM) stubs and carbon paint was applied to the circumference to avoid charging effects. The SEM stubs were sputtered with platinum to a thickness of 2 - 20 nm and analysed with a Neon focused ion beam – SEM (Zeiss) operating at 15 keV with a secondary electron detector.

Crystal size measurements

The particles on the glass disk were analysed by optical microscopy and images were taken to measure the area of COM crystals. Measurements were only undertaken in cases where the whole crystal was unobscured by other crystals. For all of the crystals meeting this criteria, regardless of size, a minimum of 60 crystals from each optical image were measured giving the area and the aspect ratio (length/width). The aspect ratio was found to have a 10 % variance. This analysis was performed using the software ImageJ®.

Analysis of nucleation rate and zeta potential

The determination of particle counts versus time through dynamic light scattering was used to assess the impact of additives on the nucleation rate. Similarly, the propensity of particles to aggregate was inferred by way of the magnitude of the measured zeta potential.

A 19.2 mL SUM solution was prepared by combining filtered water and the urinary medium (2 mL), followed by potassium phosphate (2 mL, 32.3 mM), zinc chloride (if required) and/or additive stock (depending on the test) solution, water was added if required to make to the final volume 20 mL. Sodium oxalate (0.4 mL, 0.1 M) was then added in a Teflon beaker and stirred constantly. An aliquot of the solution (approximately 2 mL) was placed in a disposable cell and analysed using the Zetasizer Nano-ZS (Malvern) at 25 °C. Measurements were recorded using a DPSS laser with an excitation wavelength 633 nm. The standard operating procedure was set with an

integration time of 10 seconds, taking 10 measurements. After recording the baseline 'counts' of the solution, stoichiometric calcium chloride was added, and a measurement was undertaken every 5 minutes. The aliquot of the solution that was removed for these analyses was then returned to the solution. This was then repeated until 20 minutes had passed (where nucleation was typically observed to peak). For each experiment, the time and the derived counts (in kilocounts per second, kcps) was recorded. Each experiment was repeated in triplicate and the presented data are the average of the three measurements with error bars associated with the standard deviation of these tests.

Finally, 25 minutes after the addition of the calcium chloride, zeta potential measurements were taken from the same experiment. These tests use a folded capillary cell, containing ~1 mL of the slurry. The instrument collects a maximum of 100 measurements and records the value only when the maximum number of measurements or concordant values are obtained. The above sequence was repeated in triplicate and the values were averaged to provide a final measurement for each additive.

Raman depth analysis

The organic molecules tested may adsorb or incorporate into the COM or COD crystals. The Raman spectroscopic instrument using a frequency-doubled NdYAG laser of wavelength 532 nm (green) of 50 mW can be focussed at different heights. Scanning through the crystals allows investigation of the signal response for the additives within the crystal. The entire particle was analysed by focusing the laser at different depths, whereby line scans were undertaken creating layers of signals that overlay to form a heatmap of signals across the z and y axis. From the heatmap the position of signals throughout the crystals can be examined which can elucidate mechanisms of inhibition of promotion. In addition, the Raman spectrum can be diagnostic of either COD or COM (where the ~1500 cm^{-1} peak is a doublet for COM and a singlet for COD).

Results and Discussion

Nucleation

Additives in pure SUM

Using the particle counts derived from the DLS analysis, the trend of the nucleation behaviour can be evaluated and compared. Figure 2 shows the particle numbers found in the presence of the macrocycle functionalised with Asp (PRAsp) at 1 mM. This figure also shows the results of the amino acid when present at a comparative four times the concertation (4 mM) – as the macrocycles contain four of the amino acids in their structure.

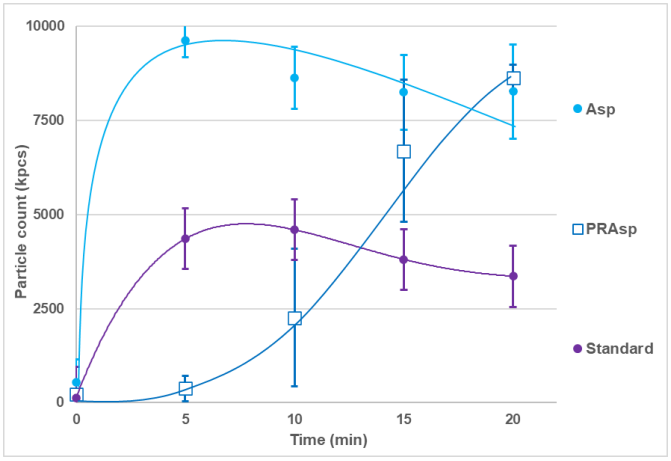

Figure 2. Particle count versus time in the presence of Asp (4 mM) and PRAsp (1 mM) in the SUM

When comparing the presence of Asp and PRAsp, it can be seen that both have final particle counts well above the standard control. There is a slower increase in particle number when PRAsp is present but eventually the particle numbers at 20 minutes are similar to when Asp is in solution. Overall, both organic molecules promote nucleation significantly above the standard, but the Asp tethered on the macrocycle slows this promotion at early stages of nucleation and then the count increases past the standard reaching is maximum around the same time period as the Asp.

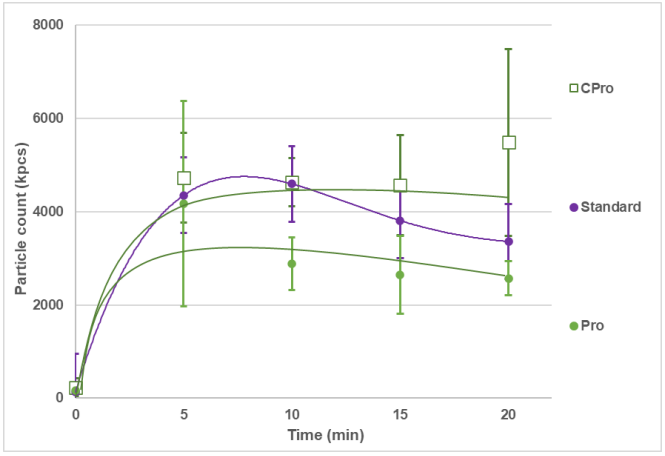

Figure 3. Particle count versus time in the presence of Pro (4 mM) and CPro (1 mM) in the SUM

Comparing the effect of CPro and the amino acid Pro (Figure 3), both are at approximately the same particle count as the standard. The resulting effect of the additives on the nucleation is very close to the standard trend; with the Pro perhaps being a mild inhibitor compared to the standard but due to the variation in the data it is hard to distinguish with confidence.

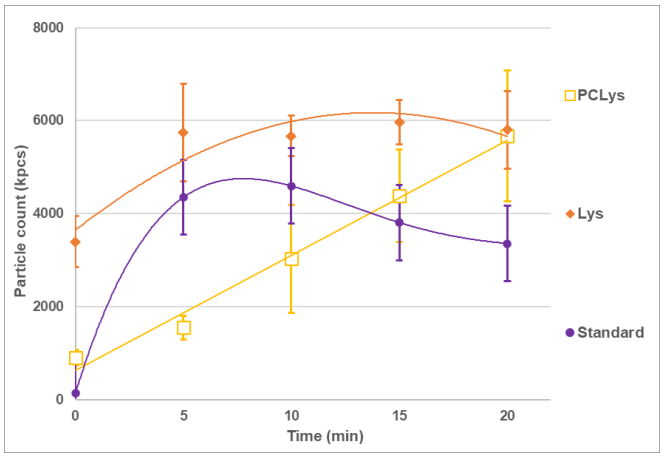

Figure 4. Particle count versus time in the presence of Lys (4 mM) and PCLys (1 mM) in the SUM

It is important to note that despite filtering right before addition, the Lys data continued to record high initial particle counts (Figure 4). This indicates that nucleation occurred quickly during the analysis, demonstrating that there is a promotion effect on the nucleation rate and overall counts. Similar to the Asp and PRAsp tests, the Lys and PCLys have an almost equal final particle count with the particle counts of both the free amino acid and calixarene being notably above the standard. Additionally, the macrocylce has slowed the nucleation rate in comparison to the free amino acid, starting much lower but eventually resulting in a similar final value.

Additives in SUM with zinc ions present

Firstly, it must be kept in mind that zinc ions lower the particle counts as can be seen in Figure 5 compared to the 'standard' in SUM (seen in the previous figures). This is because zinc ions inhibit nucleation through a lowering of the oxalate activity (through complexation with zinc ions). (30)

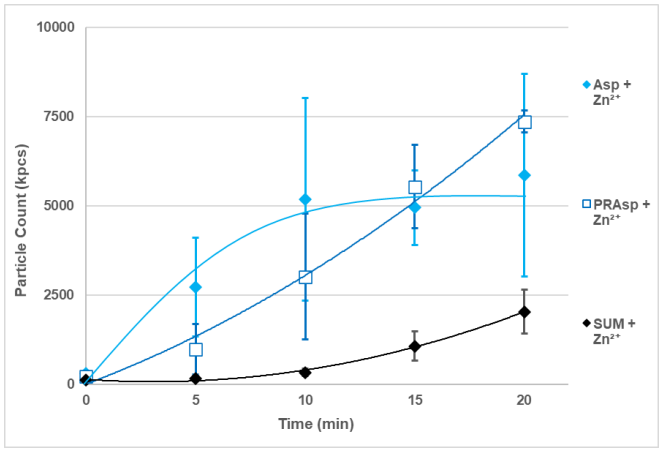

Figure 5. Particle count versus time in the presence of Asp (4 mM) and PRAsp (1 mM) in the SUM with zinc ions (1 mM)

Comparing the effect of Asp to that of PRAsp when zinc ions are also present it appears that both again are promoters (when comparing to SUM+Zn^{2+}). However, the final particle counts are higher for PRAsp than Asp when zinc ions are present (though within the variation observed for Asp). The presence of PRAsp is still seen to slow down the nucleation promotion of CaOx compared to Asp as it does not reach a peak until 20 min. Thus, the nucleation behaviour of CaOx in the presence of these additives does not appear to be impacted on by the presence or absence of zinc ions.

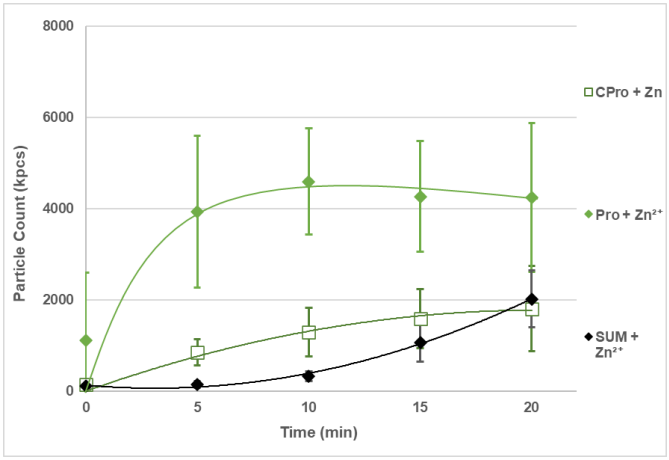

Figure 6. Particle count versus time in the presence of Pro (4 mM) and CPro (1 mM) in the SUM with zinc ions (1 mM)

The presence of Pro (Figure 6) and zinc ions shows nucleation promotion (although at 20 minutes almost within the variation of the standard measurement) while there is very minimal change to the particle count for CPro compared to SUM+Zn^{2+}. The nature of the interaction of the macrocycle appears to have changed in this case, whereby the free amino acid showed more inhibition in the absence of zinc ions. But, for the macrocycle, the zinc ions have little impact.

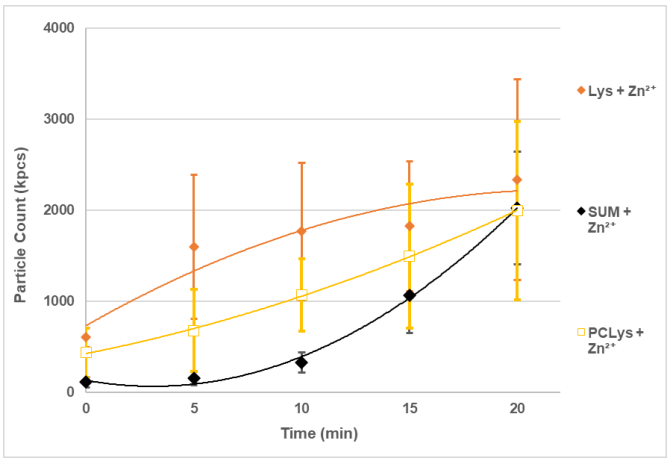

Figure 7. Particle count versus time in the presence of Lys (4 mM) and PCLys (1 mM) in the SUM with zinc ions (1 mM)

Overall, the presence of Lys and PCLys when zinc ions are also present still exhibit the behaviour of a mild promoter, especially at earlier times (Figure 7). It is interesting to note that the average trend of the macrocycle is slightly lower than that of the amino acid, which is consistent with the tests without zinc ions. Thus, little impact of zinc ions on nucleation is observed for this macrocycle.

Overall, zinc ions do not alter or have limited impact on the effect that the additives have on CaOx nucleation. This is interesting as the macrocyclic additives, and the amino acids are expected to interact with zinc ions through the carboxylic acid or amines on the molecules. For the macrocyclic additives the interaction should be more hindered than the free amino acid due to stereochemical constraints. When the amino acids are tethered to a macrocycle the nitrogen may not be able to interact in the same way. Despite this, zinc ions do not tend to alter the behaviour of the additives with respect to CaOx nucleation, though it is not clear at this point whether the additives (or zinc ions) are impacting other aspects such as morphology/hydrate form. The only notable exception to this was Pro which was more of a promoter when zinc ions were present.

Crystal Morphology

Within SUM, calcium oxalate monohydrate (COM, Figure 8a) was exclusively observed. The morphology of the COM formed within the SUM has rounded edges (see Figure S1a), through the inhibition of the (100), (021) and (121) faces, which results in a more circular morphology. This is due to the presence of citric acid in the SUM which is a well-known inhibitor of CaOx. (23,24) COD *could* be stabilised in the presence of additives and the standard morphology is shown in Figure 8b.

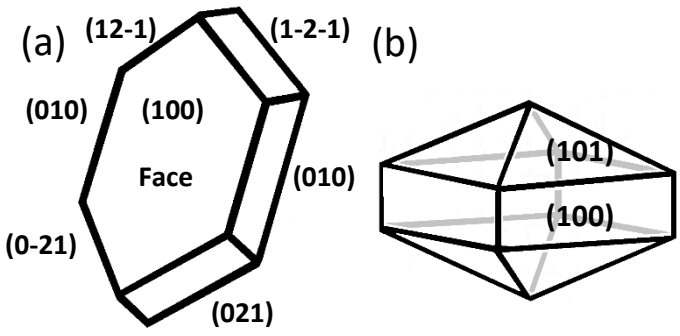

Figure 8. Schematic of (a) COM crystals forming in the presence of citric acid (19) and (b) COD morphology when forming in pure water (20)

Additional SEM images showing the particles formed in the presence of the additives with and without zinc ions can be found in the supplementary section (Figures S1, S2).

Aspartic acid functionalised propyl resorcin[4]arene (PRAsp)

Figure 9 shows the comparison in CaOx particles formed when free aspartic acid (at a comparable concentration) and the aspartic acid on the resorcin[4]arene are present. On the left it can be seen the crystals are very similar to the typical COM crystals found in SUM (Figure 8a). However, on the right it can be seen that the crystals are of a very different morphology, and, as confirmed by Raman spectroscopy (see supplementary figure S3), COD is exclusively present. The COD is also significantly elongated compared to the COD typically observed (see Figure 8b), having a very visible (100) face and having a large number of crystals forming inside of other crystals. The process of collecting crystals was more difficult as they did not stick to the glass plate. Because of this, the plate could not be rinsed off without losing all the particles.

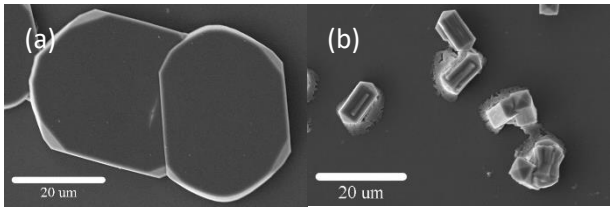

Figure 9. CaOx particles obtained in the presence of (a) aspartic acid (4 mM), and (b) PRAsp (1 mM) in SUM

The formation of COD is of interest as this typically does not occur within the standard tests. The comparison to Asp means that this is not due solely to the amino acid. Thus, the presence of PRAsp stabilises the formation of COD either by inhibiting the transition from COD to COM or by templating the formation of COD. Templating tends to effect the nucleation, leading to a longer incubation time and faster rate of nucleation (7) and this is consistent with the observed results here. These crystals have an elongated (100) face which is likely a result of the selective interaction between the macrocycle and the crystal face. Face selectivity is also observed with templating. (7) Also, of interest to note is that the size of these COD crystals is much smaller than the COM particles formed. Therefore, while the presence of Asp free or functionalised on the macrocycle increases nucleation, the CaOx crystals are smaller when the Asp is functionalised on the resorcinarene and are of a different hydrate form.

It should be noted that PRAsp could not be collected when zinc ions were present as these were accidently washed before it was realised this was an issue. During the collection method the crystals did not attach to the plate resulting in the loss of the crystals. Asp amino acid did not significantly impact the morphology of the particles (See supplementary information S2 for the SEM images of particles formed in the presence of Asp and zinc ions).

Proline functionalised Calix[4]arene (CPro)

The morphology of COM in the presence of the proline amino acid is not altered but there is an impact on the size of the formed crystals as well as on aggregation (Figure 10a) compared to the standard control (supplementary figure S1) and this is

consistent with the nucleation results discussed previously. This implies that there is some interaction of the Pro with calcium oxalate but that it is not face specific.

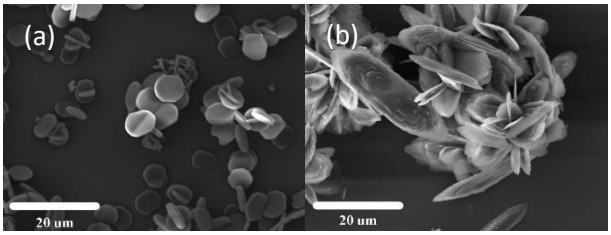

Figure 10. CaOx particles formed in the presence of (a) Pro (4 mM) and (b) CPro (1 mM) in SUM

The crystals formed in the presence of CPro are very flat and much thinner than any of the crystals formed thus far in either SUM or in the presence of any of the additives (suggesting an impact in the *a* lattice direction). Additionally, there is some visible layering and a large number of crystals growing inside of other crystals. The (100) face is the dominant face as the (021) and associated faces are not very noticeable in comparison.

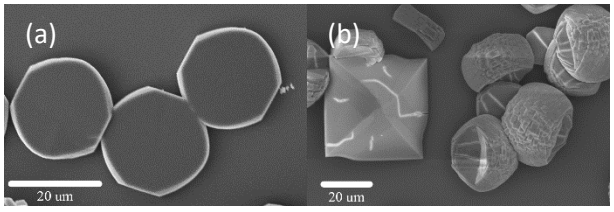

Figure 11. CaOx particles formed in the presence of (a) Pro (4 mM) + zinc ions and (b) CPro (1 mM) + zinc ions in SUM

The presence of zinc ions appears to reverse the effect on size that the Pro was seen to have in Figure 10a (Figure 11a). This is probably due to the complexation between the zinc ions and oxalate. This interaction has been recorded in previous research. (30, 35) Interestingly, the aggregation of the particles in the presence of the CPro is still visible despite the zinc ions being present although there are also COD particles observed. The layering seen in the COM particles appears thicker in the presence of zinc ions. In the presence of both the free and tethered Pro the (021) related faces all appear more dominant with rounding visible where those faces meet. However, there is less rounding with the (101) faces and they appear much better defined. This means that both the proline and CPro have impacts on the same face. When the amino acid is tethered, the CPro shows some additional interaction causing the formation of the layering effect on COM particles. The limited impact that CPro has on nucleation suggests that the CPro mainly impacts on growth processes.

Lysine functionalised propyl calix[4]arene (PCLys)

As can be seen in Figure 12, the amino acid lysine is not found to have a significant impact on the COM crystals formed. Again, the amino acid essentially reproduces the shape of the standard COM morphology in SUM.

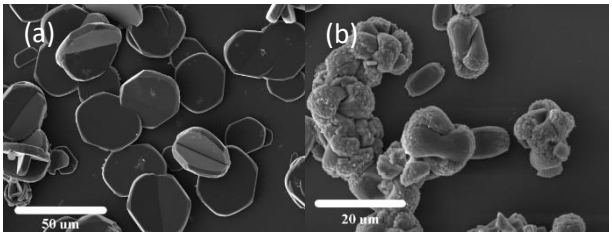

Figure 12. CaOx particles formed in the presence of (a) Lys (4 mM) and (b) PCLys (1 mM) in SUM

However, when the Lys is attached to a calix[4]arene with a propyl chain (PCLys) the crystals do not have very well-defined features. Despite this, the Raman spectrum confirms these are indeed COM particles (see supplementary figure S4). It is very hard to distinguish any faces with certainty on these crystals, the morphology is so altered compared to particles formed in both pure water and SUM. (30) What can be seen is a 'roughness' on the outside of the crystals and a large degree of aggregation of the crystals on the plate. These crystals also seem to be a lot thicker and rounder than the standard crystals.

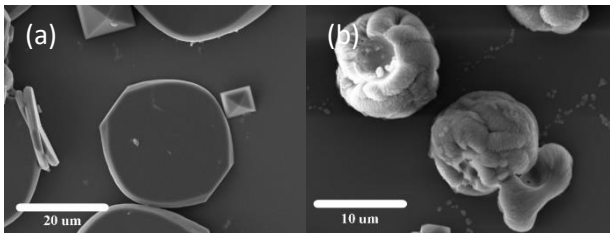

Figure 13. CaOx particles formed in the presence of (a) Lys (4 mM) + zinc ions and (b) PCLys (1 mM) + zinc ions in SUM

When zinc ions are present in addition to the Lys there is not much of a change to the COM morphology except for the stabilisation of some COD that can be seen in Figure 13a. This change in the morphology is expected from the impact of zinc ions in the medium (30). When viewing the particles formed in SUM+PCLys+Zn^{2+}, the crystals have no well-defined faces from the typical COM shape. Again, these crystals were confirmed as COM by Raman. The crystals also seem to either aggregate into or form almost spherical structures with a roughened surface. These structures also have some sort of 'indent' in the shape. This indented shape doesn't seem to be associated with a particular face, although it does appear to be reproduced in several crystals. This 'indent' can be seen in the lower right of Figure 13b. Thus, the presence of PCLys seems to greatly impact the crystal's morphology in such a way that there are no defined faces. It is difficult to tell which faces are inhibited or promoted based on these images. This unique shape could be due to some branching mechanism causing this formation outward from the initial shape. Branching however does not explain the 'indent' formed in the shape. There is more investigation needed into this system.

Crystal Size and Aspect Ratio

In Tables 3, 4 the comparison between the impacts of the amino acid functionalised macrocycles and their associated amino acids on the particle sizes can be seen. It is important to note that, where possible, the crystals measured were the individual crystals not the aggregates of the crystals.

The area of the formed crystals in the presence of aspartic acid is slightly higher than the standard, although within experimental error. The particles formed in the presence of Lys are approximately half the size of those formed in the control with those formed in the presence of Pro smaller still. The presence of the PRAsp forms COD particles and so strictly speaking the size cannot be compared to the standard or to the Asp system. Having said this, the COD particles formed in the presence of PRAsp are much smaller than the COM particles formed in the presence of Asp. The presence of CPro does form significantly smaller particles than the control although not as small as proline alone. In contrast the presence of PCLys formed even smaller particles than Lys alone.

Table 3. Recorded impact of the macromolecule additives in SUM (amino acids at 4mM, macrocycles at 1mM) on the size of CaOx formed.

Species	Area (μm^2)		
Control	910 ± 263		
Asp	1214 ± 425	PRAsp*	46 ± 14
Pro	32 ± 9	CPro	142 ± 54
Lys	583 ±140	PCLys	111 ± 27

*PRAsp produced COD crystals not COM

The smaller particle size observed in the case of PRAsp could also be due to the nucleation promotion observed, but nucleation promotion is also observed in the case of Asp and the final particle sizes are larger than the standard particles. This suggests that the presence of Asp promotes growth of COM as well as nucleation. When the Pro and CPro are present the particle counts (and hence nucleation rate) are close to the standard, but the sizes of COM particles is much smaller than the standard suggesting that growth of COM is inhibited by these additives. In the case of Lys and PCLys, nucleation was mildly promoted but the growth is significantly impacted as seen in the SEM images and the size data.

While the PRAsp could not be investigated with zinc ions present because the crystals could not be recovered from the solution the respective amino acid was still tested.

Table 4. Recorded impact of the macromolecule additives in SUM+Zn^{2+} on the size of CaOx formed (amino acids at 4mM, macrocycles at 1mM).

Species	Aspect ratio		
Control	1.23		
Asp	1.32	PRAsp	2.23
Pro	1.31	CPro	3.46
Lys	1.16	PCLys	1.81

When observing the impact on size (for the case of SUM+Zn^{2+}) the presence of the amino acids always resulted in particles which were smaller than the control with Asp forming the smallest particles for the amino acids. The particles formed in the presence of PCLys were, however, the smallest of all when zinc ions were present and significantly smaller than those of the control. For Asp the smaller particle sizes could be due to the increased nucleation, however, this cannot be the case for proline. In this case, the smaller size must be due to growth inhibition. In addition, the extent of promotion when Lys or PCLys are present cannot account for the small size that is observed when PCLys is present suggesting again that this impacts growth of COM significantly.

Table 5. Recorded impact of additives in SUM (amino acids at 4mM, macrocycles at 1mM) on the aspect ratio of CaOx formed.

Species	Area (μm^2)		
Control	1102 ± 346		
Asp	347 ± 67	PRAsp	-
Pro	420 ± 39	CPro	685 ± 14
Lys	738 ± 242	PCLys	58 ± 12

*PRAsp produced COD crystals not COM

The particles formed in the presence of the free amino acids result in similar aspect ratios; the change in the aspect ratio being at most 0.09 (and within the 10% error). The effect of the amino acids alone seems minor, although the nucleation impact of these varies, with Pro being similar to the standard and Asp being a notable promoter. The aspect ratio of CaOx particles formed in the presence of the macrocycles is significantly altered. For the PRAsp case, this is because COD particles are formed while when CPro is present this highlights the elongation of the particles. In the case of PCLys there is only a slight elongation, and the dominant change is actually in the aggregate shape.

Table 6. Recorded impact of additives in SUM+Zn^{2+} (amino acids at 4mM, macrocycles at 1mM) on the aspect ratio of CaOx.

Species	Aspect ratio		
Control	0.97		
Asp	1.19	PRAsp	-
Pro	0.98	CPro	1.18
Lys	0.98	PCLys	1.44

When comparing the effect the presence of zinc ions has on aspect ratio, again the amino acids all appear to have a similar impact. The largest difference in aspect ratio is 0.22 for the case of Asp and is the only significantly different result for the free amino acids. This means the particles formed are slightly longer than the control particles. The impact of PCLys on CaOx particles formed in the presence of zinc ions show a value of 1.44 which is larger than the control and suggests longer particles are formed. In this case, it should be noted, the aggregate shape is not being measured but any individual particles observed.

Incorporation of the additive

After analysis of the size and shape of the crystals the next step was to determine what could be occurring to give the response observed. To do this the crystals were analysed using Raman spectroscopy, where the focal point of the laser can be at different depths in the crystal giving multiple spectra for different layers through the crystals. Since different vibrational frequencies can be observed for the CaOx particles and the organic additive, this can provide a 'heatmap' for a particular signal (Figure 14), which can be highlighted to show the strength of the signal throughout the crystal. The signals chosen are typically those which are different to standard COM or COD standard spectra and compared to the COM or COD signal present. In this way, a relative region where the additive is most concentrated can be determined.

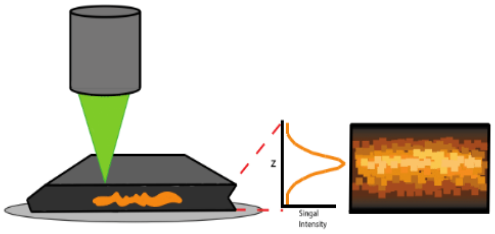

Figure 14. Depth analysis depiction providing a heatmap based on signal intensity (from ref (30))

The crystal analysed through depth analysis were required to be alone and showing the (100) basal face. For the COM crystals it was analysed from one (010) face to the other to keep the analysis consistent. For COD crystals the cross section analysis is across the (100) face without going through the (010) (supplementary figures S9-S11).

Aspartic acid functionalised propyl resorcin[4]arene (PRAsp)

The presence of the PRAsp in SUM was the only macocycle to significantly stabilise COD particles so depth analysis was performed on this system. From the spectrum obtained there was an anomalous signal with respect to the normal COD spectra showing a signal response from approximately 2800 cm^{-1} (Figure 15). The signal present there is notably different from the spectrum obtained from COD formed in the SUM (Figure S5) and based on the signal response from the additive itself (Figure S6), it is likely from the C-H stretch of the additive. Since there is no other source of C-H in the rest of the crystal this was identified as the best candidate to determine the position of the additive in the crystal.

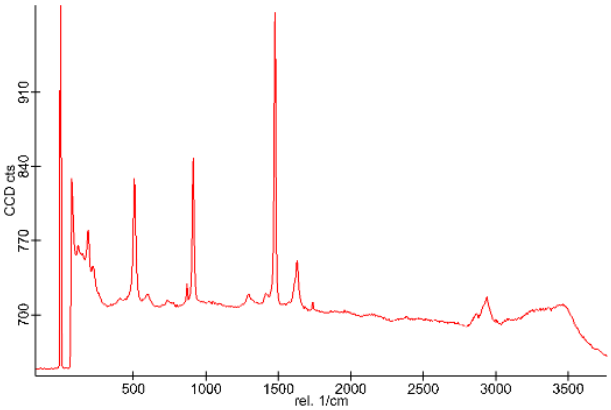

Figure 15. Signal response from the Raman depth analysis of COD in SUM with the presence of PRAsp taken as the total average throughout the crystal.

Analysing the heatmap (Figure 16) from the 2800 cm^{-1} signal compared to the signal for the C-C stretch in CaOx, it is possible to determine the relative position of the PRAsp within or on the COD crystal. It would appear (Figure 16) that the additive signal is throughout the crystal with less around the surface of the crystal. This indicates that the effect is occurring in the early stages; the PRAsp adsorbs onto the surface but is then incorporated into the crystal and stabilises the formation of COD. There is also an observed impact during the growth of the particles resulting in the elongated COD particles. It can be concluded that there is strong binding between the PRAsp with the solid allowing it to interact at all stages.

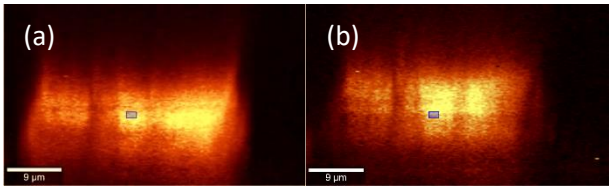

Figure 16. Heat map of the intensity of the Raman depth analysis of COD particles formed in SUM with the presence of PRAsp. (a) the COD C-C stretch signal 900 cm^{-1} is shown in comparison to (b) the signal for C-H stretch 2800 cm^{-1} . Scale bar 9 µm

Lysine functionalised propyl calix[4]arene (PCLys)

The PCLys also showed the 2800 cm^{-1} from the C-H stretch in the additive (Figure 17, supplementary figure S7) and so was used to compare to the heatmap response of the C-C stretch in COM (Figure 18). When looking at the heatmap response of the crystals the C-H stretch signal appears all throughout the crystal, including the surface. This supports the supposition that this additive is incorporating into the crystal, via initial adsorption to the surface.

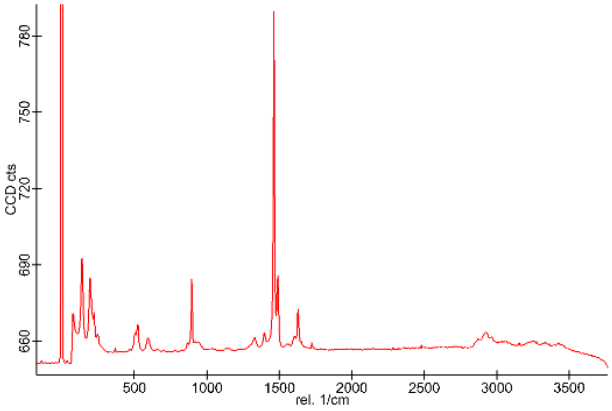

Figure 17. Signal response from the Raman depth analysis of COM in SUM with the presence of PCLys taken as the total average throughout the crystal.

From the heatmap it is obvious that there is a separation in the signal response indicating evidence of twinning, which is common in COM. Alternatively, the segmentation may be evidence of the divot visible in the micrographs (Figure 12 and 13). Thus, a strong interaction between additive and crystal is also observed, albeit with COM rather than COD. This strong interaction is likely the reason for formation of the unique structures shown in the SEM images whereby growth is significantly impacted.

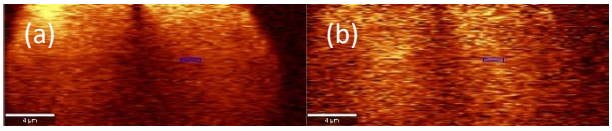

Figure 18. Heat map of the intensity of the Raman depth analysis of COM in SUM with the presence of PCLys. (a) the heat map intensity of the COM C-C stretch signal 900 cm^{-1} and (b) the signal for C-H stretch 2800 cm^{-1} . Scale bar 4 µm

Proline functionalised calix[4]arene (CPro)

As seen in Figure 19 there is a signal in the ~2800 cm^{-1} range showing evidence of the incorporation of the calixarene (supplementary figure S8) into the crystal.

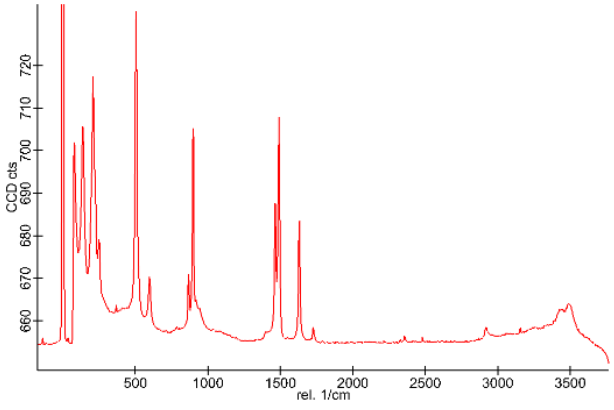

Figure 19. Signal response from the Raman depth analysis of COM in SUM with the presence of CPro taken as the total average throughout the crystal.

The heatmap response also appears to be throughout the crystal including the surface (Figure 20), showing the impact occurs throughout the whole growth of the crystallisation process.

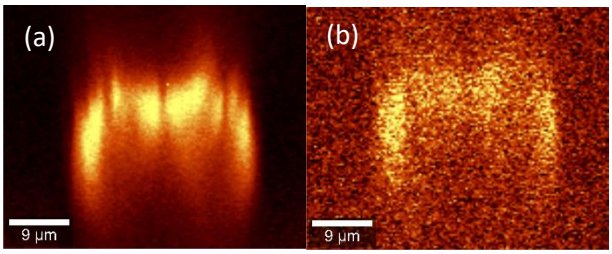

Figure 20. Heat map of the intensity of the Raman depth analysis of COM in SUM with the presence of CPro. (a) heat map intensity of the COM C-C stretch signal 900 cm^{-1} and (b) the signal for C-H stretch 2800 cm^{-1} . Scale bar 9 µm

In comparison to the other two depth analysis tests the additive response (2800 cm^{-1}) from the depth analysis shows a lesser intensity overall. Although, what is of note is the significant intensity of the signal at 3500 cm^{-1}. Considering the shape and sharpness of this signal it is unlikely that this is a response of the O-H stretch of free water. The signal is likely the response from the O-H in the lower rim of the CPro structure which isn't present in the other additives. The intensity difference is due to the overall strength of O-H signals in Raman analysis. (36)

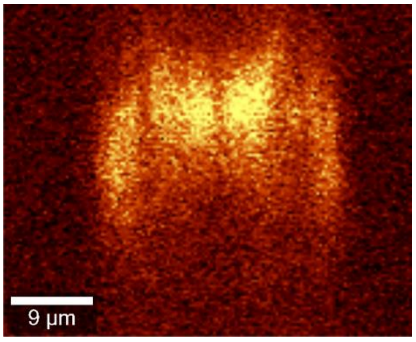

Figure 21. Heat map of the intensity of the Raman depth analysis of COM in SUM with the presence of CPro showing the signal for O-H stretch 3500 cm^{-1}

It does appear however the intensity of C-H stretches are different between the additives although the intensity of the signals is somewhat consistent with the differences in the number of C-H stretches possible from the additives. The CPro presents the lowest C-H intensity but also is the smallest molecule and contains the least C-H bonds compared to the other additives. This is predominantly due to not only the size of the amino acid but the presence of a side chain in both PCLys and PRAsp (propyl chain).

Aggregation potential

Zeta potential measures the double layer around a particle and, at low ionic strength, is related to the surface charge. More importantly, the zeta potential can give information on the likelihood of aggregation, as particles in a solution with similar surface charge should repel each other. However, it is found that generally particles with zeta potentials <±30 mV are likely

to aggregate. (5) Thus, zeta potential can give information on the likelihood of larger stone formation through an aggregative process.

The effect of PRAsp on the resulting zeta potential (Figure 22) is significantly beyond the effect of any other additive recorded in these tests. The high absolute magnitude of the zeta potential reduces the likelihood of aggregation to form larger particles. The high absolute magnitude will mean the lowest likelihood of aggregation of the particles in the presence of this molecule. In addition to charge stabilisation, these larger molecules may also sterically stabilise particles against aggregation, thus a lower zeta potential may not be as critical for these macrocyclic additives. It should be noted that the PRAsp formed COD particles and that based on these results the COD is less likely to aggregate than the COM particles formed under the tested conditions.

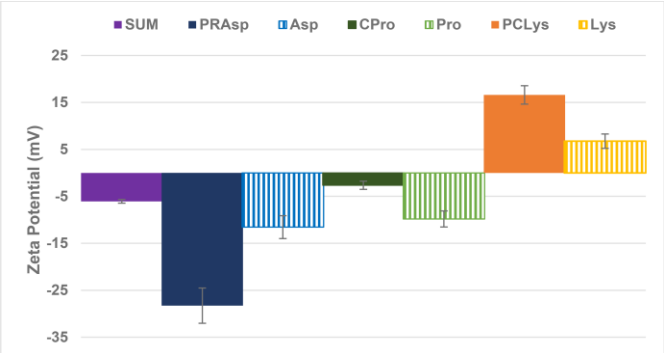

Figure 22. Effect of additives in solution on the zeta potential of CaOx crystal in SUMs; PRAsp (1 mM) (Navy), Aspartic acid (4 mM) (Blue), CPro (1 mM) (Moss), Proline (4 mM) (green), PCLys (1 mM) (Orange), Lys (4 mM) (Yellow)

This is in stark contrast to the presence of Asp which shows particles with a zeta potential closer to zero. This is likely due to the tendency for the molecule to form a zwitterion at the experimental pH. Due to the smaller magnitude of the zeta potential, when present as an additive, Asp will likely increase the tendency of particles to aggregate. This shows that the interaction is being made by the combination of the base resorcin[4]arene structure and the functionalised chemical, which leads to a significant effect on the zeta potential that is much stronger than just the Asp.

The particles formed in the presence of CPro show a zeta potential close to zero. The reason for the low zeta potential could be due to the CPro only containing four carboxylic acid groups as opposed to the 8 present in PRAsp. Alternatively, the presence of a phenolic hydroxide at the lower rim of the structure may cause some additional interaction resulting in this lower magnitude. As the phenolic hydroxyl is neutral the presence of these groups in the double layer may result in a smaller absolute value of the zeta potential. However, the Pro amino acid results in COM particles with a larger magnitude of zeta potential. Thus, the macrocyclic scaffold is impacting on this value.

The impact the presence of Lys has on zeta potential is significantly different to the other additives, displaying a positive zeta potential where the other molecules resulted in CaOx particles with a negative or slightly negative value. Also of note is the impact of the PCLys, which shows a significant increase from the amino acid response. This is similar to the impact seen with the PRAsp. In the presence of PCLys this increase means that the particles are less likely to aggregate as the magnitude is greater than 15 mV. This highly positive impact is likely due to the total absence of any carboxyl acid moiety as this molecule is functionalised though the carboxylic acid using an amide bond, leaving two free primary amines. These can then interact with the charge around the particle giving this highly positive result. This in itself is interesting due to the low concentration (1mM) of additive present compared to the other species in the SUM.

It is interesting to also note that the impact of the additives on zeta potential appears to have some relationship with the isoelectric points of the free amino acids at least in the absence of zinc ions.

It can be seen (Figure 22 and 23) that in comparison to the standard, zinc ions increase the zeta potential in magnitude but make the particle more negative. This is despite the addition of the positive ions of zinc. One possible way in which this may occur is if the zinc ions adsorb to the surface and then attract the negative counter-ions from the SUM to the particle resulting in a more negative value.

Figure 23. Effect of additives in SUM with the presence of zinc ions on the zeta potential of CaOx crystals; zinc ions in SUM (purple), PRAsp (1 mM) (navy), Aspartic acid (4 mM) (blue), CPro (1 mM) (Moss), Proline (4 mM) (green), PCLys (1 mM) (Orange), Lys (4 mM) (Yellow)

Zinc ions in the solution results in minimal change in the zeta potential of the particles formed for the CPro and Pro case, which do not result in a significantly lowered magnitude. PCLys experiences no significant change in the presence of zinc ions either, which is likely due to the molecule being positively charged and as such there is no likely interaction between zinc

ions and the calixarene. However, the presence of Asp results in a notable increase (more positive value) in the zeta potential. When both PRAsp and zinc ions are present in solution there is a significant change (~8 mV) on the measured zeta potential. This may be due to the ability of PRAsp to chelate, which could result in some of the PRAsp interacting with zinc ions in solution resulting in a less negative zeta potential from the additive when zinc ions are present.

One of the most interesting impacts of zinc ions is the effect on the Lys amino acid, where the signal changes from ~5 mV to ~ -2 mV which is the largest change present when zinc ions are introduced. This is likely due to some of the zinc ions forming complexes with lysine which has been observed previously. (37) This lowers the zeta potential of the CaOx particles but will result in the zeta potential still remaining closer to zero than the standard in SUM. The effect of chelation is not observed with PCLys, which is due to the fact that this chelation with the amino acid would occur through the carboxylic acid and primary amine site and the carboxylic acid is the functional group that is used in the coupling, making it unavailable for interaction. That is, for the PCLys, the chelation between the Zn^{2+} and the amino acid cannot occur since the amide bond was formed between the carboxylate of the amino acid and the calixarene, leaving only the amine functional groups free.

Conclusions

Calixarenes and resorcinarenes are promising scaffolds for investigation of the crystal growth modification of calcium oxalate. These amino acid functionalised molecules have shown that the large impact the additives have had on the nucleation rate, crystal growth and the zeta potential values of calcium oxalate particles formed is essentially due to the functionalisation onto the scaffold. Considering their overall interactions, the most interesting of the additives are both PCLys and PRAsp. These molecules result in calcium oxalate particles with very large zeta potentials (with and without the presence of zinc ions). This means that PCLys and PRAsp will likely have a significant impact on the aggregation of the particles – reducing this likelihood.

Additionally, PRAsp causes the stabilisation of COD in the SUM, which could make the formation of stones even more difficult. On a less positive note, the presence of PRAsp did show that nucleation is significantly promoted, however, more nucleation could lead to smaller particles that are less damaging. The presence of PCLys significantly alters the size of the crystals causing the formation of much smaller crystals. Also of note is that the crystal's morphology is very different with the faces being indistinguishable. The crystals could indicate the possibility of branching and appear to form roughly spherical aggregates. There is still much to learn about why these molecules have the impact they do but all of the additives tested showed incorporation into the crystal through the Raman depth analysis. This means that after adsorption, the additives are strongly interacting with the surface, so much so that the additive is then incorporated into the crystal. PRAsp being found less on the surface may suggest that most of this additive is already incorporated by the time the crystal is analysed.

Whilst CPro had no significant impact on the zeta potential or nucleation rates there was still a very notable impact on the morphology. The crystal form, both in the presence of the SUM and the SUM + zinc ions, show evidence of layering. Like the other additives, incorporation was also confirmed through Raman depth analysis and while the impact appears mainly on the growth processes, the interaction between additive and calcium oxalate particles is still strong enough for incorporation to occur.

Based on the analysis of all the data it seems that the additives are all likely adsorbing onto the surface of either the nuclei or the growing particles and interacting with the crystal throughout crystallisation. Using the depth analysis it can be identified that the signals for the organics are found to incorporate suggesting a very strong interaction. This strong adsorption mechanism would also explain the significant change in the size and morphology of the crystals formed as well as the significant impacts on the zeta potential.

The varied responses from the amino acid functionalised calixarenes and resorcinarenes opens up a large avenue for functionalisation and investigation of new molecules. It is especially interesting that the impact occurs despite there being very minimal impact on the crystals from the free amino acids. This may in future also give insights into the significant and varied impact of proteins. These results show crystal growth modification for calcium oxalate can be achieved at low concentrations. Thus, this data shows evidence that these molecules should be further investigated. In future, whether these macrocyclic molecules result in promising therapeutic treatments for reoccurring kidney stone formers will depend on much more research into their toxicity, bioavailability, *in-vitro* and, finally, *in-vivo* efficacy.

Author Contributions

Using the CRediT taxonomy: OB conceptualised the project, conducted the investigation, formal analysis of data and wrote the first draft. MB collected SEM data (Investigation). FJ and MM conceptualised the project, supervised and had scientific input into data interpretation (formal analysis) and writing of subsequent drafts.

Conflicts of interest

There are no conflicts to declare

Acknowledgements

We would like to acknowledge the John de Laeter Center and Curtin University facilities and equipment. We would also like to thank the Australian Government for funding via the Research Training Program scholarship.

Notes and references

1. Weiner S, Dove PM. An Overview of Biomineralization Processes and the Problem of the Vital Effect. Reviews in Mineralogy and Geochemistry. 2003;54(1):1-29.
2. Asplin JR. Hyperoxaluric calcium nephrolithiasis. Endocrinology and Metabolism Clinics of North America. 2002;31(4):927-49.
3. Frey-Wyssling A. Crystallography of the two hydrates of crystalline calcium oxalate in plants. American Journal of Botany. 1981;68(1):130-41.
4. Olafson KN, Li R, Alamani BG, Rimer JD. Engineering Crystal Modifiers: Bridging Classical and Nonclassical Crystallization. Chemistry of Materials. 2016;28(23):8453-65.
5. Maurer T, Kraushaar-Czarnetzki B. Effect of electrolyte addition on the colloidal stability of aqueous zeolite sols. Helvetica Chimica Acta. 2001;84:2550-6.
6. Martin X, Smith LH, Werness PG. Calcium oxalate dihydrate formation in urine. Kidney International. 1984;25(6):948-52.
7. Pfund LY, Price CP, Frick JJ, Matzger AJ. Controlling Pharmaceutical Crystallization with Designed Polymeric Heteronuclei. Journal of the American Chemical Society. 2015;137(2):871-5.
8. Ryall R, Fleming D, Doyle I, Evans N, Dean C, Marshall V. Intracrystalline Proteins and the Hidden Ultrastructure of Calcium Oxalate Urinary Crystals: Implications for Kidney Stone Formation. Journal of structural biology. 2001;134:5-14.
9. Sayan P, Sargut ST, Kıran B. Calcium oxalate crystallization in the presence of amino acids, proteins and carboxylic acids. Crystal Research and Technology. 2009;44(8):807-17.
10. Fleming DE, Van Riessen A, Chauvet MC, Grover PK, Hunter B, Van Bronswijk W, et al. Intracrystalline Proteins and Urolithiasis: A Synchrotron X-ray Diffraction Study of Calcium Oxalate Monohydrate. Journal of Bone and Mineral Research. 2003;18(7):1282-91.
11. Farmanesh S, Alamani BG, Rimer JD. Identifying alkali metal inhibitors of crystal growth: a selection criterion based on ion pair hydration energy. Chemical Communications. 2015;51(73):13964-7.
12. Meyer JL, Thomas WC, Jr. Trace metal-citric acid complexes as inhibitors of calcification and crystal growth. II. Effects of Fe(III), Cr(III) and Al(III) complexes on calcium oxalate crystal growth. J Urol. 1982;128(6):1376-8.
13. Aggarwal KP, Narula S, Kakkar M, Tandon C. Nephrolithiasis: molecular mechanism of renal stone formation and the critical role played by modulators. Biomed Res Int. 2013;2013:292953-.
14. Fleming DE, van Bronswijk W, Ryall RL. A comparative study of the adsorption of amino acids on to calcium minerals found in renal calculi. Clin Sci (Lond). 2001;101(2):159-68.
15. Jung T, Sheng X, Choi CK, Kim W-S, Wesson JA, Ward MD. Probing Crystallization of Calcium Oxalate Monohydrate and the Role of Macromolecule Additives with in Situ Atomic Force Microscopy. Langmuir. 2004;20(20):8587-96.
16. Wesson JA, Ward MD. Role of crystal surface adhesion in kidney stone disease. Current Opinion in Nephrology and Hypertension. 2006;15(4).
17. Golovanova OA, Punin YUO, Vysotskiy AS, Khannanov VR. Effect of Organic and Inorganic Impurities on the Nucleation of Calcium Oxalate Monohydrate. CHEMISTRY FOR SUSTAINABLE DEVELOPMENT. 2011;19(5):463-70.
18. McMulkin CJ, Massi M, Jones F. Tetrazoles: calcium oxalate crystal growth modifiers. CrystEngComm. 2015;17(13):2675-81.
19. Yu J, Tang H, Cheng B, Zhao X. Morphological control of calcium oxalate particles in the presence of poly-(styrene-alt-maleic acid). Journal of Solid State Chemistry. 2004;177(10):3368-74.
20. Jung T, Kim W-S, Kyun Choi C. Crystal structure and morphology control of calcium oxalate using biopolymeric additives in crystallization. Journal of Crystal Growth. 2005;279(1):154-62.
21. Wang L, Zhang W, Qiu SR, Zachowicz WJ, Guan X, Tang R, et al. Inhibition of calcium oxalate monohydrate crystallization by the combination of citrate and osteopontin. Journal of Crystal Growth. 2006;291(1):160-5.
22. Tsujihata M. Mechanism of calcium oxalate renal stone formation and renal tubular cell injury. International Journal of Urology. 2008;15(2):115-20.
23. Siddiqui AA, Sultana T, Buchholz N-P, Waqar MA, Talati J. Proteins in renal stones and urine of stone formers. Urological Research. 1998;26(6):383-8.
24. Zisman AL. Effectiveness of Treatment Modalities on Kidney Stone Recurrence. Clinical Journal of the American Society of Nephrology. 2017;12(10):1699.
25. Yousaf A, Hamid SA, Bunnori NM, Ishola AA. Applications of calixarenes in cancer chemotherapy: facts and perspectives. Drug Des Devel Ther. 2015;9:2831-8.
26. Baldini L, Casnati A, Sansone F. Multivalent and Multifunctional Calixarenes in Bionanotechnology. European Journal of Organic Chemistry. 2020;2020(32):5056-69.
27. Neri P, Sessler JL, Wang M-X. Calixarenes and beyond: Springer; 2016.
28. Bartlett M, Mocerino M, Ogden M, Oliveira A, Parkinson G, Pettersen J, et al. Amino acid modified calixarenes as crystal growth modifiers. Journal Of Materials Science & Technology. 2005;21:1-5.
29. Español ES, Villamil MM. Calixarenes: Generalities and Their Role in Improving the Solubility, Biocompatibility, Stability, Bioavailability, Detection, and Transport of Biomolecules. Biomolecules. 2019;9(3).
30. Bottrill O, Boon M, Barker T, Jones F. Calcium oxalate crystallization in synthetic urinary medium: The impact of a more complex solution medium, organic molecules and zinc ions. Journal of Crystal Growth. 2021;553:125940.
31. Jones F, Mocerino M, Ogden MI, Oliveira A, Parkinson GM. Bio-Inspired Calix[4]arene Additives for Crystal Growth Modification of Inorganic Materials. Crystal Growth & Design. 2005;5(6):2336-43.
32. Alamani BG, Gale JD, Rimer JD. Zinc Ions Modify Calcium Oxalate Growth by Distinct Transformation of Crystal Surface Termination. Crystal Growth & Design. 2021;21(6):3375-83.
33. Brown P, Ackermann D, Finlayson B. Calcium oxalate dihydrate (weddellite) precipitation. Journal of crystal growth. 1989;98(3):285-92.
34. Sandström B. Diagnosis of Zinc Deficiency and Excess in Individuals and Populations. Food and Nutrition Bulletin. 2001;22(2):133-7.
35. Barker T, Boon M, Jones F. The role of zinc ions in calcium oxalate monohydrate crystallization. Journal of Crystal Growth. 2020;546:125777.
36. Wiley JH, Atalla RH. Band assignments in the raman spectra of celluloses. Carbohydrate Research. 1987;160:113-29.
37. Bampidis V, Azimonti G, Bastos MdL, Christensen H, Dusemund B, Kouba M, et al. Safety and efficacy of zinc chelates of lysine and

glutamic acid as feed additive for all animal species. EFSA Journal. 2019;17(7):e05782.